



Published in final edited form as:

Genes Chromosomes Cancer. 2021 October ; 60(10): 695–708. doi:10.1002/gcc.22979.

Targeted RNA Sequencing in the Routine Clinical Detection of Fusion Genes in Salivary Gland Tumors

Justin Bubola^{1,2}, Christina M. MacMillan^{1,3}, Elizabeth G. Demicco^{1,3}, Rose A. Chami^{3,4}, Catherine T-S Chung^{3,4}, Iona Leong^{1,2,3}, Paula Marrano⁴, Zeynep Onkal¹, David Swanson¹, Brandon M. Veremis⁵, Ilan Weinreb^{3,6}, Lei Zhang⁷, Cristina R. Antonescu⁷, Brendan C. Dickson^{1,3}

¹. Department of Pathology and Laboratory Medicine, Mount Sinai Hospital, Toronto, ON, Canada

². Faculty of Dentistry, University of Toronto, Toronto, ON, Canada

³. Department of Laboratory Medicine and Pathobiology, University of Toronto, Toronto,

⁴. Division of Pathology, Department of Paediatric Laboratory Medicine, The Hospital for Sick Children and University of Toronto, Toronto, ON, Canada

⁵. Department of Pathology, Mount Sinai Hospital, New York, NY, USA

⁶. Department of Pathology, University Health Network, Toronto, ON, Canada

⁷. Department of Pathology, Memorial Sloan Kettering Cancer Center, New York, NY

Abstract

Salivary gland tumors represent a diverse group of neoplasms that occasionally pose a diagnostic challenge for pathologists, particularly with limited sampling. Gene fusions, which may reflect genetic drivers, are increasingly recognized in a subset of these neoplasms, and can be leveraged for diagnostic purposes. We performed a retrospective analysis on a cohort of 80 benign and malignant salivary gland tumors, enriched for subtypes known to harbor recurrent fusion events, to validate the diagnostic use of a targeted RNA sequencing assay to detect fusion transcripts. Testing identified fusion genes in 71% (24/34) of pleomorphic adenoma and carcinoma-ex-pleomorphic adenoma, with 56% of cases showing rearrangement of *PLAG1* and 15% *HMGA2*. In addition to confirming known partners for these genes, novel *PLAG1* fusion partners were identified, including *DSTN*, *NTF3* and *MEG3*; *CNOT2* was identified as a novel fusion partner for *HMGA2*. In adenoid cystic carcinoma, 95% of cases (19/20) were positive for a fusion event. *MYB* was rearranged in 60% (12/20), *MYBL1* in 30% (6/20) and *NFIB* in 5% (1/20); two tumors exhibited novel fusion products, including *NFIB-TBPL1* and *MYBL1-VCPIPI*. Fusion genes were identified in 64% (9/14) of cases of mucoepidermoid carcinoma; *MAML2* was confirmed to partner with either *CRTC1* (43%), or *CRTC3* (21%). One salivary duct carcinoma was found to harbor a novel *RAPGEF6-ACSL6* fusion gene. Finally, as anticipated, gene fusions were not detected in any of the five acinic cell carcinomas included in the cohort. In summary, targeted

Corresponding Author: Brendan C. Dickson, MD, MSc, FRCPC, Pathology & Laboratory Medicine, Mount Sinai Hospital, 600 University Ave, Suite 6A 120.02, Toronto, Ontario, Canada M5G 1X5, P: 416.586.4800, F: 416.586.8628, Brendan.Dickson@sinaihealth.ca.

Conflicts of interest: none

RNA sequencing represents a diagnostically useful ancillary technique for identifying a variety of existing, and novel, fusion transcripts in the classification of salivary gland neoplasms.

Keywords

salivary gland tumor; fusion; RNA sequencing

INTRODUCTION

Salivary gland tumors are uncommon and represent a diverse group of neoplasms with over 30 distinct entities recognized in the current edition of the World Health Organization (WHO) Classification of Head and Neck Tumors.¹ These can present a diagnostic challenge to pathologists, particularly in the context of limited sampling, due to their rarity, morphologic heterogeneity, and overlapping cellular compositions and immunoprofiles. Indeed, differentiation between benign and malignant neoplasms can be challenging, particularly in the oral cavity where benign neoplasms, such as pleomorphic adenoma, may lack a delineating capsule. An ability to make this distinction is essential owing to differences in biologic potential and treatment.

Salivary gland tumors are increasingly recognized as frequently containing recurrent fusion genes, which has allowed diagnostic refinement and improved classification. To date, gene fusions have been identified in pleomorphic adenoma (*PLAG1*, *HMG2*),^{2–9} mucoepidermoid carcinoma (*CRTC1/CRTC3-MAML2*),^{10–13} adenoid cystic carcinoma (*MYB/MYBL1-NFIB*),^{14–16} secretory carcinoma (*ETV6-NTRK3/RET/MET/MAML3*),^{17–19} hyalinizing clear cell carcinoma (*EWSR1-ATF1/CREM*),^{20,21} the cribriform variant of polymorphous adenocarcinoma (*PRKD1/PRKD2/PRKD3*),²² acinic cell carcinoma (*NR4A3, HTN3-MSANTD3*),^{23–25} intraductal carcinoma (*RET-NCOA4/TRIM27/TRIM33/KIAA1217, TUT1-ETV5, STRN/EML4/MYO18A-ALK*)^{26–33} and myoepithelial carcinoma (*PLAG1*).^{34,35} In addition, microsecretory adenocarcinoma, which has recently been proposed as a new entity, is characterized by a novel *MEF2C-SS18* fusion gene.³⁶ It should also be noted that other forms of recurrent genetic events have also been reported in salivary gland neoplasms. For example, a minority harbor point mutations, such as basal cell adenomas (*CTNNB1*),^{37,38} sialadenoma papilliferum (*BRAFV600E*)³⁹ and the majority of the classical variant of polymorphous adenocarcinomas harbor a recurrent hotspot mutation (*PRKD1 E710D*).⁴⁰

Conventional cytogenetics has traditionally guided the identification of translocations. This was supplanted with the introduction of fluorescence in situ hybridization (FISH) and reverse transcriptase-polymerase chain reaction (RT-PCR)-based assays. Due to its specificity and potential breadth in coverage, targeted RNA sequencing (RNA-Seq) would appear to offer a practical approach to fusion gene detection, particularly for entities in which a variety of variant gene fusions have been described. This technique is now routinely employed, for example, for fusion gene detection in mesenchymal neoplasms.⁴¹ In this study we examined a cohort of salivary gland neoplasms, enriched for those with gene

fusions, with a commercially available targeted RNA-Seq assay to assess the potential of this technique as a diagnostic adjunct.

MATERIALS AND METHODS

Case Selection

Following institutional Research Ethics Board approval, a retrospective archive review was performed for benign and malignant salivary gland neoplasms (2015–2020), which included biopsy and resection specimens. The original slides were pulled and reviewed to confirm the diagnosis and select a representative block for RNA-Seq.

RNA Sequencing

Targeted RNA sequencing was performed on all cases. RNA was extracted from formalin-fixed, paraffin-embedded (FFPE) tissue scrolls (3 to 4 per case, cut at 10 μ m) using the ExpressArt FFPE Clear RNA Ready kit (Amsbio, Cambridge, MA). RNA fragment length was assessed using the RNA 6000 chip on an Agilent Bioanalyzer (Agilent Technologies, Santa Clara, CA). RNA-seq libraries were prepared using an input of 20 to 100 ng total RNA with the TruSight RNA Fusion Panel (Illumina, San Diego, CA), an enrichment-based assay that targets 507 known fusion-associated genes. Each sample was sequenced with 76 base-pair paired-end reads on an Illumina MiSeq platform at 8 samples per flow cell (~3 million reads per sample). The results were analyzed using both the STAR and BOWTIE2 aligners, and Manta and JAFFA fusion callers, respectively.

Fluorescence in situ hybridization

The application of FISH in this study was two-fold: (1) It was used to independently validate the presence of fusion gene rearrangement in tumors containing novel fusion transcripts. (2) The entire MEC sub-cohort was examined to draw a comparison of the sensitivity between FISH and RNA-Seq.

Fluorescence in situ hybridization was performed as previously reported.⁴² Briefly, custom probes were made from bacterial artificial chromosome (BAC) clones flanking the specific genes of interest based on the UCSC genome browser (<http://genome.ucsc.edu>). They were obtained from BACPAC sources of Children's Hospital of Oakland Research Institute (Oakland, Ca: <https://bacpacresources.org>). The DNA from the BACs was isolated according to the manufacturer's instructions and then labeled with fluorochromes (fluorescent-labeled dUTPs, Enzo Life Sciences, New York NY) by nick translation and subsequently validated on normal metaphase chromosomes. 4 μ m-thick tissue sections were cut from the FFPE tissue blocks to prepare the slides, which were then deparaffinized, pretreated and hybridized with the denatured probes. After allowing for an overnight incubation, the slides were rinsed and stained with 4',6-diamidino-2-phenylindole. The slides were then mounted with an anti-fade solution and examined using a Zeiss fluorescence microscope (Zeiss Axioplan, Oberkochen, Germany) and using Isis 5 software (Metasystems). (Supplementary Table 1).

Immunohistochemistry

Previously constructed tissue microarrays (TMAs)⁴³ containing 437 salivary gland tumours were investigated using immunohistochemistry (IHC) for MYB (clone: EP769Y; Abcam #ab45150); Pan-Trk (clone: EPR17341; Abcam #ab181560); and, HMGA2 (polyclonal; Biocheck, 59170AP). Tissue sections were cut at 4 µm thickness and stained using a Dako OMNIS autostainer (Alignet, Santa Clara, CA, USA) as per the manufacturer's instructions. Any nuclear staining in the tumor cells was recorded as a positive result, while non-specific cytoplasmic staining was considered negative (Supplementary Table 2).

RESULTS

Cohort

A total of 83 tumors were identified. Three cases were excluded due to failure to meet minimum RNA quality control standards, including one case that had undergone decalcification due to bone involvement. The final cohort consisted of a total of 80 cases. There were 49 females and 31 males, with an average patient age of 53 years (range: 9–96) (Table 1). The cases included pleomorphic adenoma (PA; n = 27), carcinoma-ex pleomorphic adenoma (CA-ex-PA; n = 7), mucoepidermoid carcinoma (MEC; n = 14), adenoid cystic carcinoma (AdCC; n = 20), acinic cell carcinoma (AcCC; n = 5), hyalinizing clear cell carcinoma (HCCC; n = 3), secretory carcinoma (SC; n = 2), *de novo* salivary duct carcinoma (SDC; n = 1), and intraductal carcinoma (IC; n = 1). Of the CA-ex-PAs, the malignant component was not classified in two cases, the remainder included one each of: minimally invasive carcinoma, low-grade adenocarcinoma, intracapsular carcinoma, poorly differentiated carcinoma, and SDC.

The anatomic location of the tumors included the parotid gland (n = 42), oral cavity (n = 17), submandibular gland (n = 6), sinonasal tract (n = 5), metastases (n = 3; brain, vertebrae, cervical lymph node), lacrimal gland, nasopharynx, larynx, orbit, base of tongue, neck NOS and an unspecified site (n = 1 each). In terms of the nature of specimens, 62 were resections or excisions and 18 were incisional or core biopsies. The mean tumor size was 2.8 cm for the PAs and CA-ex-PAs (range: 1.2 – 5.9 cm), 2.6 cm for the MECs (0.6 – 5.9 cm), 2.8 cm for the AdCCs (range: 1.1 – 5.9 cm) and 2.0 cm for AcCCs (range: 0.6 – 3.9 cm).

RNA Sequencing

In most cases RNA-Seq revealed fusion products that had previously been established in the literature, as well as several novel fusion products (Table 2; Figure 1).

Overall, the prevalence of fusion transcripts in the PAs and CA-ex-PAs was 71% (24/34), with 56% (19/34) involving *PLAG1* and 15% (5/34) involving *HMGA2* (Figures 1 and 2). The number of supporting reads for *PLAG1*-rearranged tumors (range = 2–162; median = 19.5) was lower than those of *HMGA2*-rearranged cases (range = 2–759; median = 215.5). Of the benign PAs, 67% (18/27) were found to contain fusion genes, with a prevalence of 56% (15/27) and 11% (3/27) for *PLAG1* and *HMGA2* rearrangement, respectively. The most common *PLAG1* fusion partner was *CTNNB1* (n = 6), followed by *NCALD* (n = 3), *LIFR*, *CHCHD7*, *ACTA2* and *FBXO32* (n = 1, each). Novel *PLAG1* fusion partners

included *DSTN* and *NTF3* (n = 1 each). The most common *HMGA2* fusion partner was *WIFI* (n = 3). Additionally, two PAs contained heretofore undescribed fusion transcripts (*PRB2-TAF15* and *NPM1-PRB2*); however, based on a low number of supporting reads, and breakpoints involving partial exons, these were discounted as stochastic events. Of the seven CA-ex-PAs in our cohort, there was a prevalence of 57% (4/7) and 29% (2/7) of *PLAG1* and *HMGA2* rearrangements, respectively. Novel *MEG3-PLAG1* and *HMGA2-CNOT2* fusion transcripts were found in two cases.

The prevalence of detectable fusion transcripts in AdCC was found to be 95% (19/20); 60% (12/20) contained the *MYB-NFIB* fusion, and 25% (5/20) the *MYBL1-NFIB* fusion (Figures 1 and 3). In addition, two cases were found to harbor novel fusion genes (*NFIB-TBPL1* and *MYBL1-VCPIP1*). In general, the AdCCs exhibited a high number of supporting reads (range = 2–1336; median = 200).

In MEC the prevalence of the *CRTC1-MAML2* fusion gene was 43% (6/14), while 21% (3/14) contained the *CRTC3-MAML2* fusion (Figures 1 and 4). Fusion transcripts were detected in 57% (4/7) of low-grade tumors, 67% (2/3) of intermediate-grade tumors, and none (0/1) of the high-grade tumors; the three remaining MECs in this sub-cohort included a clear cell variant, an oncocytic variant and a metastatic tumor which therefore did not receive a histologic grade. Overall, MECs contained a somewhat lower number of supporting reads by RNA-Seq (range = 1–11; median = 7) compared to other salivary carcinomas tested.

The remainder of the cohort consisted of five AcCCs, three HCCC, two SCs, one IC and one SDC. None of the AcCCs exhibited a fusion transcript, while 67% (2/3) of the HCCC harbored an *EWSR1-ATF1* fusion gene, both SCs harbored an *ETV6-NTRK3* fusion and the one IC harbored a *NCOA4-RET* fusion (Figure 1). The *de novo* SDC was found to contain a novel *RAPGEF6-ACSL6* fusion gene, which was in-frame; however, the significance of this finding is unknown and the possibility it may represent a secondary or stochastic event cannot be entirely excluded.

In terms of specimen type, 66% (41/62) of excision/resection specimens and 94% (17/18) of the incisional/core biopsy specimens were positive for fusion transcripts. The excision/resection specimens exhibited a range of 1–759 supporting reads (median = 26), while the incisional/core biopsies specimens had a range of 2–1336 supporting reads (median = 67). For 18% (14/80) of the tumors identified in our archival review, RNA-Seq had been employed as a diagnostic adjunct to assist in initial classification. This included PA (four cases) CA-ex-PA (one case), AdCCs (four cases), MEC (two cases), HCCC (two cases), and SC (one case).

Fluorescence in situ hybridization

FISH independently confirmed fusion gene rearrangement in all cases, apart from Case 4, which was negative for *PLAG1* rearrangement, and Case 33, which was found to show *HMGA2* amplification. Examination of the entire MEC sub-cohort by FISH showed *MAML2* rearrangement in 80% (12/15) of cases (Table 2), including three cases with

undetectable rearrangement by RNA-Seq and one case that was excluded based on insufficient quality RNA.

Immunohistochemistry

MYB IHC was found to have a sensitivity of 48.4% (45/93) and specificity of 93.6% (322/344) for AdCC. Interestingly, a distinctive abluminal or myoepithelial pattern was noted in three AdCCs with positive immunostaining for MYB. Nuclear Pan-Trk immunostaining demonstrated a sensitivity of 58.8% (10/17) and specificity of 89.5% (376/420) in the diagnosis of SC, with scattered positivity also seen in 17 mucoepidermoid carcinomas, 7 polymorphous adenocarcinomas, 5 squamous cell carcinomas, 3 adenoid cystic carcinomas, 2 intraductal carcinomas, 2 epithelial-myoepithelial carcinomas, 2 salivary duct carcinomas and 1 acinic cell carcinoma, amongst others. As the TMAs were largely composed of malignant salivary gland tumors, an accurate assessment of the sensitivity and specificity of the HMGA2 stain was not possible.

DISCUSSION:

Recurrent chromosomal translocations yielding fusion genes are commonplace in neoplasms of hematopoietic and mesenchymal origin; these are also increasingly recognized in tumors of epithelial origin, including salivary gland neoplasms.^{2-9,44} Next generation sequencing has contributed to an unparalleled rate of novel fusion gene discovery. While this offers insight into the molecular pathogenesis of these neoplasms, these genetic events can also be leveraged for diagnostic purposes. The purpose of this study was to validate a targeted RNA-Seq assay for fusion detection in salivary gland tumors.

The t(3;8)(p21;q12) translocation, resulting in a *PLAG1-CTNNB1* fusion gene, is the most common fusion event observed in pleomorphic adenoma.³ Other reported *PLAG1* fusion partners in this context include: *LIFR*, *TCEA1*, *CHCHD7*, *FGFR1*, *FBXO32*, *C1orf116*, and *NFIB*.^{2,4-6,45-47} A subset of PAs have 12q15 translocations resulting in *HMGA2* rearrangement; this gene has been reported to partner with *FHIT*, *NFIB* and *WIFI*.⁷⁻⁹ Unsurprisingly, similar gene rearrangements have also been detected in carcinoma ex-pleomorphic adenomas, including salivary duct carcinoma (SDC) ex-PA and myoepithelial carcinoma ex-PA.⁴⁸⁻⁵² Interestingly, *PLAG1* rearrangements have likewise been documented in a subset of apparently *de novo* SDC and myoepithelial carcinomas.^{35,49,53}

In this study PA / CA-ex-PA were found to have detectable fusion transcripts in 71% of cases; *PLAG1* was rearranged in 56%, and *HMGA2* in 15%. This appears similar, if not slightly better, to reports in the literature that suggest rearrangement of *PLAG1* in approximately 58% (range = 24–85 %), and *HMGA2* in about 7% (range = 2–13%) of cases.^{48-50,52-55} Novel *PLAG1* fusion partners were also identified by RNA-Seq and included single cases with *DSTN* and *MEG3* partners; and, one tumor was found to have a novel *HMGA2-CNOT2* fusion transcript. One case was found to harbour *NTF3-PLAG1* which has recently been identified in oncocyctic myoepithelioma.⁴⁷ In addition, *NCALD-PLAG1* (n = 3) and *ACTA2-PLAG1* (n = 1) gene products were identified in this sub-cohort; to date, the *NCALD-PLAG1* fusion has only been reported in a myoepithelial

carcinoma ex-PA, while the *ACTA2-PLAG1* fusion has only been documented in a *de novo* myoepithelial carcinoma.⁵³ These cases highlight the molecular overlap that exists between PA and myoepithelial neoplasms of salivary gland origin. Finally, one CA-ex-PA was found to contain a *PLAG1-NFIB* fusion transcript, which was only recently reported in a case of benign PA.⁴⁶

Adenoid cystic carcinoma is characterized by a recurrent t(6;9)(q22-23;p23-24) translocation that results in a *MYB-NFIB* fusion gene.^{14,56} An alternative *MYBL1-NFIB* gene fusion has been reported in a subset of cases.^{15,16,57} Various other genes have been reported to substitute for *MYB*, *MYBL1* and *NFIB*, including *TGFRB3*, *RAD51B*, *YTHDF3*, *AIG1*, *XRCC4* and *PTPRD*, amongst others.^{15,16,58-60} In our cohort of 20 AdCCs, the *MYB-NFIB* fusion was identified in 60% and the *MYBL1-NFIB* fusion in 25%, while two cases harbored novel *NFIB-TBPL1* and *MYBL1-VCPIP1* fusion products. A review of the literature revealed a prevalence of 60% (range = 40–86%) for *MYB* rearrangement and 13% (8–24%) for *MYBL1* rearrangement in AdCC.^{15,16,60-68}

In our archival review, we identified four AdCCs in which RNA-Seq had been employed at the time of diagnosis to facilitate classification. The initial differential diagnosis for cases 36, 51 and 54 included AdCC, polymorphous adenocarcinoma, and adenocarcinoma, not otherwise specified. RNA-Seq identified *MYBL1-NFIB*, *NFIB-TBPL1*, and *MYBL1-VCPIP1* fusion transcripts, respectively, supporting the diagnosis of AdCC in these three tumors. Case 37 presented as a nasopharyngeal mass in which the differential diagnosis included AdCC and HPV-related multiphenotypic sinonasal carcinoma with extension into the nasopharynx. Detection of the *MYB-NFIB* fusion transcript confirmed the diagnosis as AdCC. Additionally, two of the fusion-positive tumors in our cohort exhibited a solid growth pattern and high-grade transformation, respectively, highlighting how RNA-Seq may serve as a diagnostic adjunct in tumors lacking a prototypic morphology.

The majority of MECs are characterized by a t(11;19)(q21;p13) translocation, resulting in a *CRTC1-MAML2* fusion gene;¹⁰⁻¹² a subset are reported to harbor a *CRTC3-MAML2* gene fusion.¹³ Detection of these fusion products are particularly helpful in the diagnosis of histologic variants of MEC. For example, in our cohort, both the clear cell variant (Case 65) and the oncocytic variant of MEC (Case 56) initially posed a diagnostic challenge. In both cases RNA-Seq had been used at the time of initial diagnosis, with the presence of *MAML2* rearrangement supporting classification as MEC. RNA sequencing was helpful in resolving differential diagnoses in other cases as well. This is likewise the instance with Case 60, which had a variant morphology that mimicked HCCC. In contrast, Case 70 presented as a metastatic clear cell tumor in a cervical lymph node with a differential diagnosis that included the clear cell variant of MEC, HCCC and squamous cell carcinoma with clear cell change; the identification of an *EWSR1-ATF1* fusion transcript enabled definitive classification as HCCC. And, Case 67 exhibited a predominantly cystic architecture with a bland epithelial lining, which mimicked a benign cystic lesion (i.e., mucous retention cyst) on the incisional biopsy. These cases reinforce how molecular testing can be successfully employed as a diagnostic adjunct in morphologically challenging variants of MEC.

Overall, fusion products were identified in 64% of MECs; *MAML2* was partnered with *CRTC1* in 43% and *CRTC3* in 21% of cases. In comparison, a review of the literature suggests a prevalence of *MAML2* rearrangement in 52% of MEC (range = 34–82%), with 5% (range = 2–6%) of cases exhibiting a *CRTC3* fusion partner.^{13,69–78} The considerable variability in the reports of incidence of *MAML2*-rearrangement appears to be largely technique dependent. Noda *et al* (2013) previously noted the limitations of RT-PCR for fusion detection in these tumors due to comparatively low expression of fusion transcripts,⁷⁵ suggesting FISH might offer a diagnostic advantage. We likewise noted a low number of supporting reads in this group by RNA-Seq and, for this reason, decided to examine this entire subcohort by FISH. This revealed *MAML2* rearrangement in 80% (12/15). Three tumors that were negative for fusion products by RNA-Seq were found to have *MAML2* rearrangement by FISH (Cases 55, 57 and 62); conversely, one tumor was negative for *MAML2* rearrangement by FISH but positive by RNA-Seq (Case 68). In addition, one case that had been excluded based on insufficient quality RNA was examined by FISH and found to show *MAML2* rearrangement. The raw data files for the aforementioned cases were subsequently re-examined and confirmed to lack any missed fusion calls. This confirms that, while RNA-seq can frequently identify fusions in MECs, FISH generally appears to show somewhat greater sensitivity.

Recurrent molecular alterations have only recently been reported in AcCC. Novel *HTN3-MSANTD3* gene fusions have been described in a subset of AcCC, with 4.4–8% of cases showing *MSANTD3* aberrations.^{23–25} A recurrent t(4;9)(q13;q31) translocation transferring the enhancer regions of the highly expressed *SCPP* gene cluster to a location upstream of the *NR4A3* gene has also been reported.^{25,79} Consistent with the enhancer hijacking mechanism underlying this molecular finding, this rearrangement does not result in a chimeric gene fusion. Therefore, unsurprisingly none of the AcCC in our cohort were found to contain fusion transcripts by RNA-Seq.

While IHC offers a convenient and inexpensive alternative to molecular testing, these markers were found to have limited sensitivity in our hands compared to pre-existing reports in the literature. Application of IHC for MYB was found to have a sensitivity of 48.4% in the TMA for AdCC, compared to prior studies showing 64.9–82.4% sensitivity.^{61,62} Moreover, nuclear staining for Pan-Trk had a sensitivity of 58.8% for the diagnosis of SC, whereas the literature describes Pan-Trk IHC as having a sensitivity ranging from 64–74%.^{80–82} The decreased sensitivity of Pan-Trk may, in part, be attributable to the presence of non-*NTRK3* fusion partners in a subset of cases. Additionally, while the EPR17341 Pan-Trk clone recognizes an amino acid sequence that conserved across all three Trk proteins, its sensitivity for *NTRK3* fusion-positive tumors has been shown to be less than its sensitivity for detecting *NTRK1* and *NTRK2* fusion-positive tumors.⁸³ Pan-Trk expression has also been described as focal and weak in a subset of *NTRK3*-positive tumors, with some cases exhibiting less than 5% of tumor cells staining,⁸³ which might lead to false negative interpretation with the limited sampling inherent to TMA cores. Finally, for both stains, the reduced sensitivity in this study may be potentiated by the age of the tumors incorporated into the TMA, many of which being over 10 years old.

In summary, targeted RNA-Seq represents a useful diagnostic technique for fusion gene detection in salivary gland neoplasms. In addition to confirming the presence of known gene fusions, it also has the advantage of enabling identification of novel fusion partners, thereby also refining understanding of the molecular pathogenesis of these neoplasms. RNA-Seq was able to successfully detect fusion transcripts in both excision/resection specimens as well as incisional/core biopsy specimens. Cost and turnaround time notwithstanding, a potential limitation of this assay included an inability to detect certain molecular alterations such as the enhancer rearrangements seen in AcCCs, as well as missing fusions in a subset of cases with low copy expression (i.e., MEC). It is possible that with more comprehensive panels, and greater sequencing depth, the detection rate of these events will increase in the future. In the meantime, as this technology gains broader traction in clinical laboratories, RNA-Seq offers an important adjunct in the diagnosis of this diverse group of neoplasms.

Supplementary Material

Refer to Web version on PubMed Central for supplementary material.

Funding:

Panov 2 Research Fund

Data Availability Statement:

Available from corresponding author upon reasonable request.

References:

1. El-Naggar A, Chan J, Grandis J, Takata T, Slootweg P. WHO Classification of Head and Neck Tumours. 4th ed. Lyon: International Agency for Research on Cancer; 2017.
2. Aström AK, Voz ML, Kas K, et al. Conserved mechanism of PLAG1 activation in salivary gland tumors with and without chromosome 8q12 abnormalities: identification of SII as a new fusion partner gene. *Cancer Res.* 1999;59(4):918–923. [PubMed: 10029085]
3. Kas K, Voz ML, Röijer E, et al. Promoter swapping between the genes for a novel zinc finger protein and beta-catenin in pleiomorphic adenomas with t(3;8)(p21;q12) translocations. *Nat Genet.* 1997;15(2):170–174. [PubMed: 9020842]
4. Voz ML, Aström AK, Kas K, Mark J, Stenman G, Van de Ven WJ. The recurrent translocation t(5;8)(p13;q12) in pleomorphic adenomas results in upregulation of PLAG1 gene expression under control of the LIFR promoter. *Oncogene.* 1998;16(11):1409–1416. [PubMed: 9525740]
5. Asp J, Persson F, Kost-Alimova M, Stenman G. CHCHD7-PLAG1 and TCEA1-PLAG1 gene fusions resulting from cryptic, intrachromosomal 8q rearrangements in pleomorphic salivary gland adenomas. *Genes Chromosomes Cancer.* 2006;45(9):820–828. [PubMed: 16736500]
6. Persson F, Winnes M, André Y, et al. High-resolution array CGH analysis of salivary gland tumors reveals fusion and amplification of the FGFR1 and PLAG1 genes in ring chromosomes. *Oncogene.* 2008;27(21):3072–3080. [PubMed: 18059337]
7. Geurts JM, Schoenmakers EF, Röijer E, Stenman G, Van de Ven WJ. Expression of reciprocal hybrid transcripts of HMGIC and FHIT in a pleomorphic adenoma of the parotid gland. *Cancer Res.* 1997;57(1):13–17. [PubMed: 8988031]
8. Geurts JM, Schoenmakers EF, Röijer E, Aström AK, Stenman G, van de Ven WJ. Identification of NFIB as recurrent translocation partner gene of HMGIC in pleomorphic adenomas. *Oncogene.* 1998;16(7):865–872. [PubMed: 9484777]

9. Queimado L, Lopes CS, Reis AM. WIF1, an inhibitor of the Wnt pathway, is rearranged in salivary gland tumors. *Genes Chromosomes Cancer*. 2007;46(3):215–225. [PubMed: 17171686]
10. Nordkvist A, Gustafsson H, Juberg-Ode M, Stenman G. Recurrent rearrangements of 11q14–22 in mucoepidermoid carcinoma. *Cancer Genet Cytogenet*. 1994;74(2):77–83. [PubMed: 8019965]
11. Tonon G, Modi S, Wu L, et al. t(11;19)(q21;p13) translocation in mucoepidermoid carcinoma creates a novel fusion product that disrupts a Notch signaling pathway. *Nat Genet*. 2003;33(2):208–213. [PubMed: 12539049]
12. Enlund F, Behboudi A, Andrén Y, et al. Altered Notch signaling resulting from expression of a WAMTP1-MAML2 gene fusion in mucoepidermoid carcinomas and benign Warthin's tumors. *Exp Cell Res*. 2004;292(1):21–28. [PubMed: 14720503]
13. Fehr A, Röser K, Heidorn K, Hallas C, Löning T, Bullerdiek J. A new type of MAML2 fusion in mucoepidermoid carcinoma. *Genes Chromosomes Cancer*. 2008;47(3):203–206. [PubMed: 18050304]
14. Persson M, Andrén Y, Mark J, Horlings HM, Persson F, Stenman G. Recurrent fusion of MYB and NFIB transcription factor genes in carcinomas of the breast and head and neck. *Proc Natl Acad Sci U S A*. 2009;106(44):18740–18744. [PubMed: 19841262]
15. Mitani Y, Liu B, Rao PH, et al. Novel MYBL1 Gene Rearrangements with Recurrent MYBL1-NFIB Fusions in Salivary Adenoid Cystic Carcinomas Lacking t(6;9) Translocations. *Clin Cancer Res*. 2016;22(3):725–733. [PubMed: 26631609]
16. Brayer KJ, Frerich CA, Kang H, Ness SA. Recurrent Fusions in MYB and MYBL1 Define a Common, Transcription Factor-Driven Oncogenic Pathway in Salivary Gland Adenoid Cystic Carcinoma. *Cancer Discov*. 2016;6(2):176–187. [PubMed: 26631070]
17. Skálová A, Vanecek T, Sima R, et al. Mammary analogue secretory carcinoma of salivary glands, containing the ETV6-NTRK3 fusion gene: a hitherto undescribed salivary gland tumor entity. *Am J Surg Pathol*. 2010;34(5):599–608. [PubMed: 20410810]
18. Skalova A, Vanecek T, Martinek P, et al. Molecular Profiling of Mammary Analog Secretory Carcinoma Revealed a Subset of Tumors Harboring a Novel ETV6-RET Translocation: Report of 10 Cases. *Am J Surg Pathol*. 2018;42(2):234–246. [PubMed: 29076873]
19. Guilmette J, Dias-Santagata D, Nosé V, Lennerz JK, Sadow PM. Novel gene fusions in secretory carcinoma of the salivary glands: enlarging the ETV6 family. *Hum Pathol*. 2019;83:50–58. [PubMed: 30130630]
20. Antonescu CR, Katabi N, Zhang L, et al. EWSR1-ATF1 fusion is a novel and consistent finding in hyalinizing clear-cell carcinoma of salivary gland. *Genes Chromosomes Cancer*. 2011;50(7):559–570. [PubMed: 21484932]
21. Chapman E, Skalova A, Ptakova N, et al. Molecular Profiling of Hyalinizing Clear Cell Carcinomas Revealed a Subset of Tumors Harboring a Novel EWSR1-CREM Fusion: Report of 3 Cases. *Am J Surg Pathol*. 2018;42(9):1182–1189. [PubMed: 29975250]
22. Weinreb I, Zhang L, Tirunagari LM, et al. Novel PRKD gene rearrangements and variant fusions in cribriform adenocarcinoma of salivary gland origin. *Genes Chromosomes Cancer*. 2014;53(10):845–856. [PubMed: 24942367]
23. Andreasen S, Varma S, Barasch N, et al. The HTN3-MSANTD3 Fusion Gene Defines a Subset of Acinic Cell Carcinoma of the Salivary Gland. *Am J Surg Pathol*. 2019;43(4):489–496. [PubMed: 30520817]
24. Barasch N, Gong X, Kwei KA, et al. Recurrent rearrangements of the Myb/SANT-like DNA-binding domain containing 3 gene (MSANTD3) in salivary gland acinic cell carcinoma. *PLoS One*. 2017;12(2):e0171265. [PubMed: 28212443]
25. Haller F, Bieg M, Will R, et al. Enhancer hijacking activates oncogenic transcription factor NR4A3 in acinic cell carcinomas of the salivary glands. *Nat Commun*. 2019;10(1):368. [PubMed: 30664630]
26. Skálová A, Vanecek T, Uro-Coste E, et al. Molecular Profiling of Salivary Gland Intraductal Carcinoma Revealed a Subset of Tumors Harboring NCOA4-RET and Novel TRIM27-RET Fusions: A Report of 17 cases. *Am J Surg Pathol*. 2018;42(11):1445–1455. [PubMed: 30045065]

27. Skálová A, Ptáková N, Santana T, et al. NCOA4-RET and TRIM27-RET Are Characteristic Gene Fusions in Salivary Intraductal Carcinoma, Including Invasive and Metastatic Tumors: Is “Intraductal” Correct? *Am J Surg Pathol.* 2019;43(10):1303–1313. [PubMed: 31162284]
28. Weinreb I, Bishop JA, Chiosea SI, et al. Recurrent RET Gene Rearrangements in Intraductal Carcinomas of Salivary Gland. *Am J Surg Pathol.* 2018;42(4):442–452. [PubMed: 29443014]
29. Lu H, Graham RP, Seethala R, Chute D. Intraductal Carcinoma of Salivary Glands Harboring TRIM27-RET Fusion with Mixed Low Grade and Apocrine Types. *Head Neck Pathol.* 2020;14(1):239–245. [PubMed: 30610524]
30. Rooper LM, Thompson LDR, Gagan J, Oliari BR, Weinreb I, Bishop JA. Salivary Intraductal Carcinoma Arising within Intraparotid Lymph Node: A Report of 4 Cases with Identification of a Novel STRN-ALK Fusion. *Head Neck Pathol.* 2020.
31. Majewska H, Gorczycki A, Czapiewski P, et al. ALK alterations in salivary gland carcinomas. *Virchows Arch.* 2021;478(5):933–941. [PubMed: 33237469]
32. Bishop JA, Nakaguro M, Whaley RD, et al. Oncocytic intraductal carcinoma of salivary glands: a distinct variant with TRIM33-RET fusions and BRAF V600E mutations. *Histopathology.* 2020.
33. Agaimy A, Baníková M, Ihrlér S, et al. ALK Rearrangements Characterize 2 Distinct Types of Salivary Gland Carcinomas: Clinicopathologic and Molecular Analysis of 4 Cases and Literature Review. *Am J Surg Pathol.* 2021.
34. Skálová A, Weinreb I, Hycza M, et al. Clear cell myoepithelial carcinoma of salivary glands showing EWSR1 rearrangement: molecular analysis of 94 salivary gland carcinomas with prominent clear cell component. *Am J Surg Pathol.* 2015;39(3):338–348. [PubMed: 25581728]
35. Skálová A, Agaimy A, Vanecek T, et al. Molecular Profiling of Clear Cell Myoepithelial Carcinoma of Salivary Glands With EWSR1 Rearrangement Identifies Frequent PLAG1 Gene Fusions But No EWSR1 Fusion Transcripts. *Am J Surg Pathol.* 2020.
36. Bishop JA, Weinreb I, Swanson D, et al. Microsecretory Adenocarcinoma: A Novel Salivary Gland Tumor Characterized by a Recurrent MEF2C-SS18 Fusion. *Am J Surg Pathol.* 2019;43(8):1023–1032. [PubMed: 31094920]
37. Jo VY, Sholl LM, Krane JF. Distinctive Patterns of CTNNB1 (β -Catenin) Alterations in Salivary Gland Basal Cell Adenoma and Basal Cell Adenocarcinoma. *Am J Surg Pathol.* 2016;40(8):1143–1150. [PubMed: 27259009]
38. Lee YH, Huang WC, Hsieh MS. CTNNB1 mutations in basal cell adenoma of the salivary gland. *J Formos Med Assoc.* 2018;117(10):894–901. [PubMed: 29224720]
39. Hsieh MS, Bishop JA, Wang YP, et al. Salivary Sialadenoma Papilliferum Consists of Two Morphologically, Immunophenotypically, and Genetically Distinct Subtypes. *Head Neck Pathol.* 2020;14(2):489–496. [PubMed: 31473937]
40. Weinreb I, Piscuoglio S, Martelotto LG, et al. Hotspot activating PRKD1 somatic mutations in polymorphous low-grade adenocarcinomas of the salivary glands. *Nat Genet.* 2014;46(11):1166–1169. [PubMed: 25240283]
41. Dickson BC, Swanson D. Targeted RNA sequencing: A routine ancillary technique in the diagnosis of bone and soft tissue neoplasms. *Genes Chromosomes Cancer.* 2019;58(2):75–87. [PubMed: 30350361]
42. Kao YC, Sung YS, Zhang L, et al. EWSR1 Fusions With CREB Family Transcription Factors Define a Novel Myxoid Mesenchymal Tumor With Predilection for Intracranial Location. *Am J Surg Pathol.* 2017;41(4):482–490. [PubMed: 28009602]
43. Bishop JA, Koduru P, Veremis BM, et al. SS18 Break-Apart Fluorescence In Situ Hybridization is a Practical and Effective Method for Diagnosing Microsecretory Adenocarcinoma of Salivary Glands. *Head Neck Pathol.* 2021.
44. Bullerdiek J, Wobst G, Meyer-Bolte K, et al. Cytogenetic subtyping of 220 salivary gland pleomorphic adenomas: correlation to occurrence, histological subtype, and in vitro cellular behavior. *Cancer Genet Cytogenet.* 1993;65(1):27–31. [PubMed: 8381711]
45. Chen T, Wehrs R, Raslan S, et al. Identification of a Novel Fusion Transcript Involving F-box Protein 32 (FBXO32) and Pleomorphic Adenoma Gene 1 (PLAG1) in Pleomorphic Adenoma. *Modern Pathology.* 2018;31:474. [PubMed: 29052596]

46. Kakay Afshari M, Fehr A, Tejera Nevado P, Andersson MK, Stenman G. Activation of PLAG1 and HMGA2 by gene fusions involving the transcriptional regulator gene NFIB. *Genes Chromosomes Cancer*. 2020.
47. Ban ková M, Uro-Coste E, Ptáková N, et al. What is hiding behind S100 protein and SOX10 positive oncocytomas? Oncocytic pleomorphic adenoma and myoepithelioma with novel gene fusions in a subset of cases. *Hum Pathol*. 2020;103:52–62. [PubMed: 32673681]
48. Bahrami A, Dalton JD, Shivakumar B, Krane JF. PLAG1 alteration in carcinoma ex pleomorphic adenoma: immunohistochemical and fluorescence in situ hybridization studies of 22 cases. *Head Neck Pathol*. 2012;6(3):328–335. [PubMed: 22485045]
49. Katabi N, Ghossein R, Ho A, et al. Consistent PLAG1 and HMGA2 abnormalities distinguish carcinoma ex-pleomorphic adenoma from its de novo counterparts. *Hum Pathol*. 2015;46(1):26–33. [PubMed: 25439740]
50. Asahina M, Saito T, Hayashi T, Fukumura Y, Mitani K, Yao T. Clinicopathological effect of PLAG1 fusion genes in pleomorphic adenoma and carcinoma ex pleomorphic adenoma with special emphasis on histological features. *Histopathology*. 2019;74(3):514–525. [PubMed: 30307055]
51. Persson F, Andrén Y, Winnes M, et al. High-resolution genomic profiling of adenomas and carcinomas of the salivary glands reveals amplification, rearrangement, and fusion of HMGA2. *Genes Chromosomes Cancer*. 2009;48(1):69–82. [PubMed: 18828159]
52. Andreasen S, von Holstein SL, Homøe P, Heegaard S. Recurrent rearrangements of the PLAG1 and HMGA2 genes in lacrimal gland pleomorphic adenoma and carcinoma ex pleomorphic adenoma. *Acta Ophthalmol*. 2018;96(7):e768–e771. [PubMed: 29437290]
53. Dalin MG, Katabi N, Persson M, et al. Multi-dimensional genomic analysis of myoepithelial carcinoma identifies prevalent oncogenic gene fusions. *Nat Commun*. 2017;8(1):1197. [PubMed: 29084941]
54. Martins C, Fonseca I, Roque L, et al. PLAG1 gene alterations in salivary gland pleomorphic adenoma and carcinoma ex-pleomorphic adenoma: a combined study using chromosome banding, in situ hybridization and immunocytochemistry. *Mod Pathol*. 2005;18(8):1048–1055. [PubMed: 15920557]
55. Matsuyama A, Hisaoka M, Nagao Y, Hashimoto H. Aberrant PLAG1 expression in pleomorphic adenomas of the salivary gland: a molecular genetic and immunohistochemical study. *Virchows Arch*. 2011;458(5):583–592. [PubMed: 21394649]
56. Stenman G, Sandros J, Dahlenfors R, Juberg-Ode M, Mark J. 6q- and loss of the Y chromosome--two common deviations in malignant human salivary gland tumors. *Cancer Genet Cytogenet*. 1986;22(4):283–293. [PubMed: 3015376]
57. Šteiner P, Andreasen S, Grossmann P, et al. Prognostic significance of 1p36 locus deletion in adenoid cystic carcinoma of the salivary glands. *Virchows Arch*. 2018;473(4):471–480. [PubMed: 29619555]
58. Mitani Y, Rao PH, Futreal PA, et al. Novel chromosomal rearrangements and break points at the t(6;9) in salivary adenoid cystic carcinoma: association with MYB-NFIB chimeric fusion, MYB expression, and clinical outcome. *Clin Cancer Res*. 2011;17(22):7003–7014. [PubMed: 21976542]
59. Drier Y, Cotton MJ, Williamson KE, et al. An oncogenic MYB feedback loop drives alternate cell fates in adenoid cystic carcinoma. *Nat Genet*. 2016;48(3):265–272. [PubMed: 26829750]
60. Rettig EM, Talbot CC, Sausen M, et al. Whole-Genome Sequencing of Salivary Gland Adenoid Cystic Carcinoma. *Cancer Prev Res (Phila)*. 2016;9(4):265–274. [PubMed: 26862087]
61. Brill LB, Kanner WA, Fehr A, et al. Analysis of MYB expression and MYB-NFIB gene fusions in adenoid cystic carcinoma and other salivary neoplasms. *Mod Pathol*. 2011;24(9):1169–1176. [PubMed: 21572406]
62. West RB, Kong C, Clarke N, et al. MYB expression and translocation in adenoid cystic carcinomas and other salivary gland tumors with clinicopathologic correlation. *Am J Surg Pathol*. 2011;35(1):92–99. [PubMed: 21164292]
63. Persson M, Andrén Y, Moskaluk CA, et al. Clinically significant copy number alterations and complex rearrangements of MYB and NFIB in head and neck adenoid cystic carcinoma. *Genes Chromosomes Cancer*. 2012;51(8):805–817. [PubMed: 22505352]

64. Ho AS, Kannan K, Roy DM, et al. The mutational landscape of adenoid cystic carcinoma. *Nat Genet.* 2013;45(7):791–798. [PubMed: 23685749]
65. Rettig EM, Tan M, Ling S, et al. MYB rearrangement and clinicopathologic characteristics in head and neck adenoid cystic carcinoma. *Laryngoscope.* 2015;125(9):E292–299. [PubMed: 25963073]
66. Fujii K, Murase T, Beppu S, et al. MYB, MYBL1, MYBL2 and NFIB gene alterations and MYC overexpression in salivary gland adenoid cystic carcinoma. *Histopathology.* 2017;71(5):823–834. [PubMed: 28594149]
67. Frerich CA, Brayer KJ, Painter BM, et al. Transcriptomes define distinct subgroups of salivary gland adenoid cystic carcinoma with different driver mutations and outcomes. *Oncotarget.* 2018;9(7):7341–7358. [PubMed: 29484115]
68. Togashi Y, Dobashi A, Sakata S, et al. MYB and MYBL1 in adenoid cystic carcinoma: diversity in the mode of genomic rearrangement and transcripts. *Mod Pathol.* 2018;31(6):934–946. [PubMed: 29410490]
69. Okabe M, Miyabe S, Nagatsuka H, et al. MECT1-MAML2 fusion transcript defines a favorable subset of mucoepidermoid carcinoma. *Clin Cancer Res.* 2006;12(13):3902–3907. [PubMed: 16818685]
70. Miyabe S, Okabe M, Nagatsuka H, et al. Prognostic significance of p27Kip1, Ki-67, and CRTC1-MAML2 fusion transcript in mucoepidermoid carcinoma: a molecular and clinicopathologic study of 101 cases. *J Oral Maxillofac Surg.* 2009;67(7):1432–1441. [PubMed: 19531414]
71. Nakayama T, Miyabe S, Okabe M, et al. Clinicopathological significance of the CRTC3-MAML2 fusion transcript in mucoepidermoid carcinoma. *Mod Pathol.* 2009;22(12):1575–1581. [PubMed: 19749740]
72. Seethala RR, Dacic S, Ciepły K, Kelly LM, Nikiforova MN. A reappraisal of the MECT1/MAML2 translocation in salivary mucoepidermoid carcinomas. *Am J Surg Pathol.* 2010;34(8):1106–1121. [PubMed: 20588178]
73. Chiosea SI, Dacic S, Nikiforova MN, Seethala RR. Prospective testing of mucoepidermoid carcinoma for the MAML2 translocation: clinical implications. *Laryngoscope.* 2012;122(8):1690–1694. [PubMed: 22833306]
74. Clauditz TS, Gontarewicz A, Wang CJ, et al. 11q21 rearrangement is a frequent and highly specific genetic alteration in mucoepidermoid carcinoma. *Diagn Mol Pathol.* 2012;21(3):134–137. [PubMed: 22847156]
75. Noda H, Okumura Y, Nakayama T, et al. Clinicopathological significance of MAML2 gene split in mucoepidermoid carcinoma. *Cancer Sci.* 2013;104(1):85–92. [PubMed: 23035786]
76. Luk PP, Wykes J, Selinger CI, et al. Diagnostic and prognostic utility of Mastermind-like 2 (MAML2) gene rearrangement detection by fluorescent in situ hybridization (FISH) in mucoepidermoid carcinoma of the salivary glands. *Oral Surg Oral Med Oral Pathol Oral Radiol.* 2016;121(5):530–541. [PubMed: 27068311]
77. Saade RE, Bell D, Garcia J, Roberts D, Weber R. Role of CRTC1/MAML2 Translocation in the Prognosis and Clinical Outcomes of Mucoepidermoid Carcinoma. *JAMA Otolaryngol Head Neck Surg.* 2016;142(3):234–240. [PubMed: 26796488]
78. Birkeland AC, Foltin SK, Michmerhuizen NL, et al. Correlation of Crtc1/3-Mam12 fusion status, grade and survival in mucoepidermoid carcinoma. *Oral Oncol.* 2017;68:5–8. [PubMed: 28438292]
79. Haller F, Skálová A, Ihrler S, et al. Nuclear NR4A3 Immunostaining Is a Specific and Sensitive Novel Marker for Acinic Cell Carcinoma of the Salivary Glands. *Am J Surg Pathol.* 2019;43(9):1264–1272. [PubMed: 31094928]
80. Bell D, Ferrarotto R, Liang L, et al. Pan-Trk immunohistochemistry reliably identifies ETV6-NTRK3 fusion in secretory carcinoma of the salivary gland. *Virchows Arch.* 2020;476(2):295–305. [PubMed: 31423558]
81. Xu B, Haroon Al Rasheed MR, Antonescu CR, et al. Pan-Trk immunohistochemistry is a sensitive and specific ancillary tool for diagnosing secretory carcinoma of the salivary gland and detecting ETV6-NTRK3 fusion. *Histopathology.* 2020;76(3):375–382.
82. Hung YP, Jo VY, Hornick JL. Immunohistochemistry with a pan-TRK antibody distinguishes secretory carcinoma of the salivary gland from acinic cell carcinoma. *Histopathology.* 2019;75(1):54–62. [PubMed: 30801752]

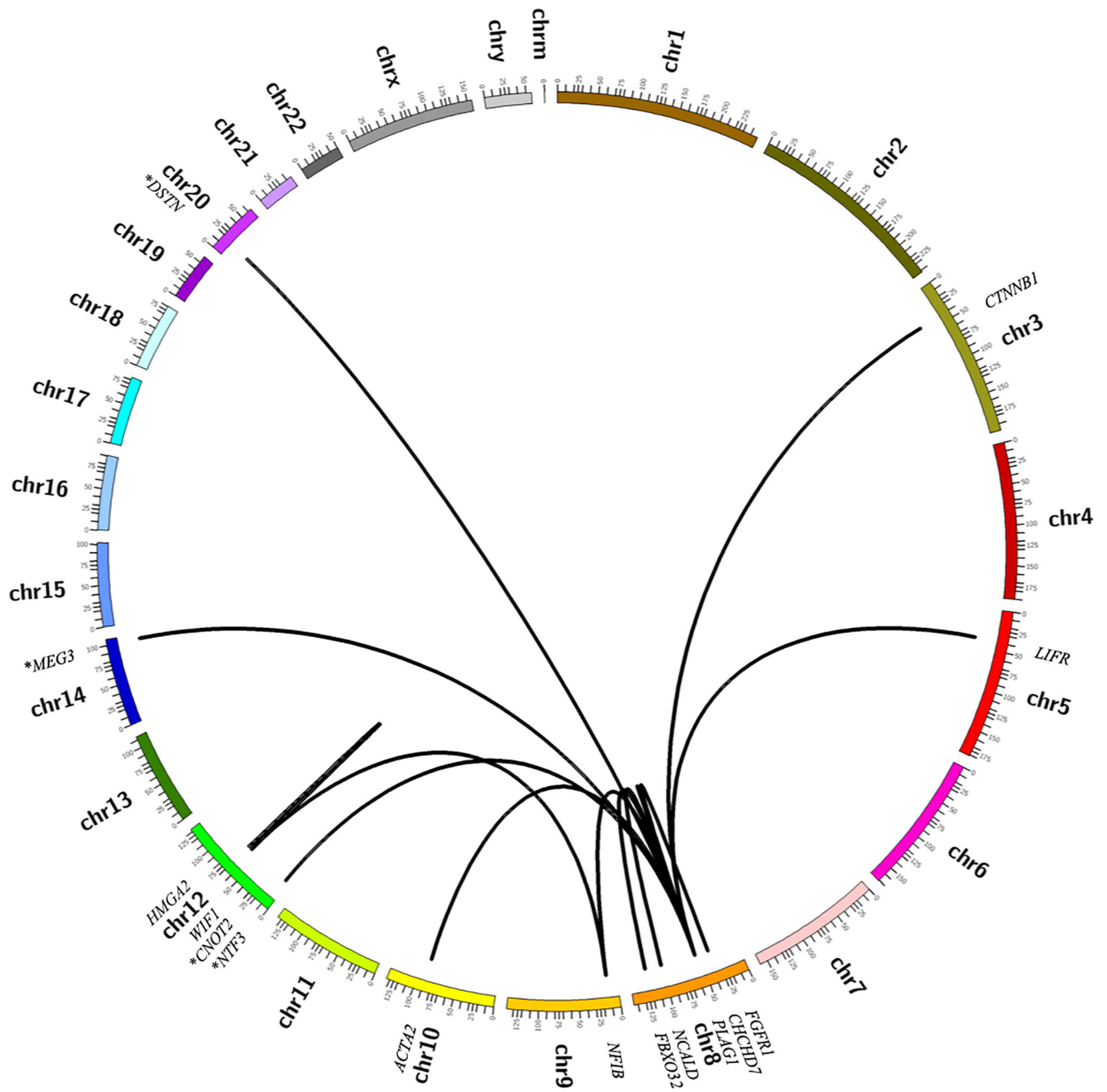
83. Solomon JP, Linkov I, Rosado A, et al. NTRK fusion detection across multiple assays and 33,997 cases: diagnostic implications and pitfalls. *Mod Pathol.* 2020;33(1):38–46. [PubMed: 31375766]

Author Manuscript

Author Manuscript

Author Manuscript

Author Manuscript



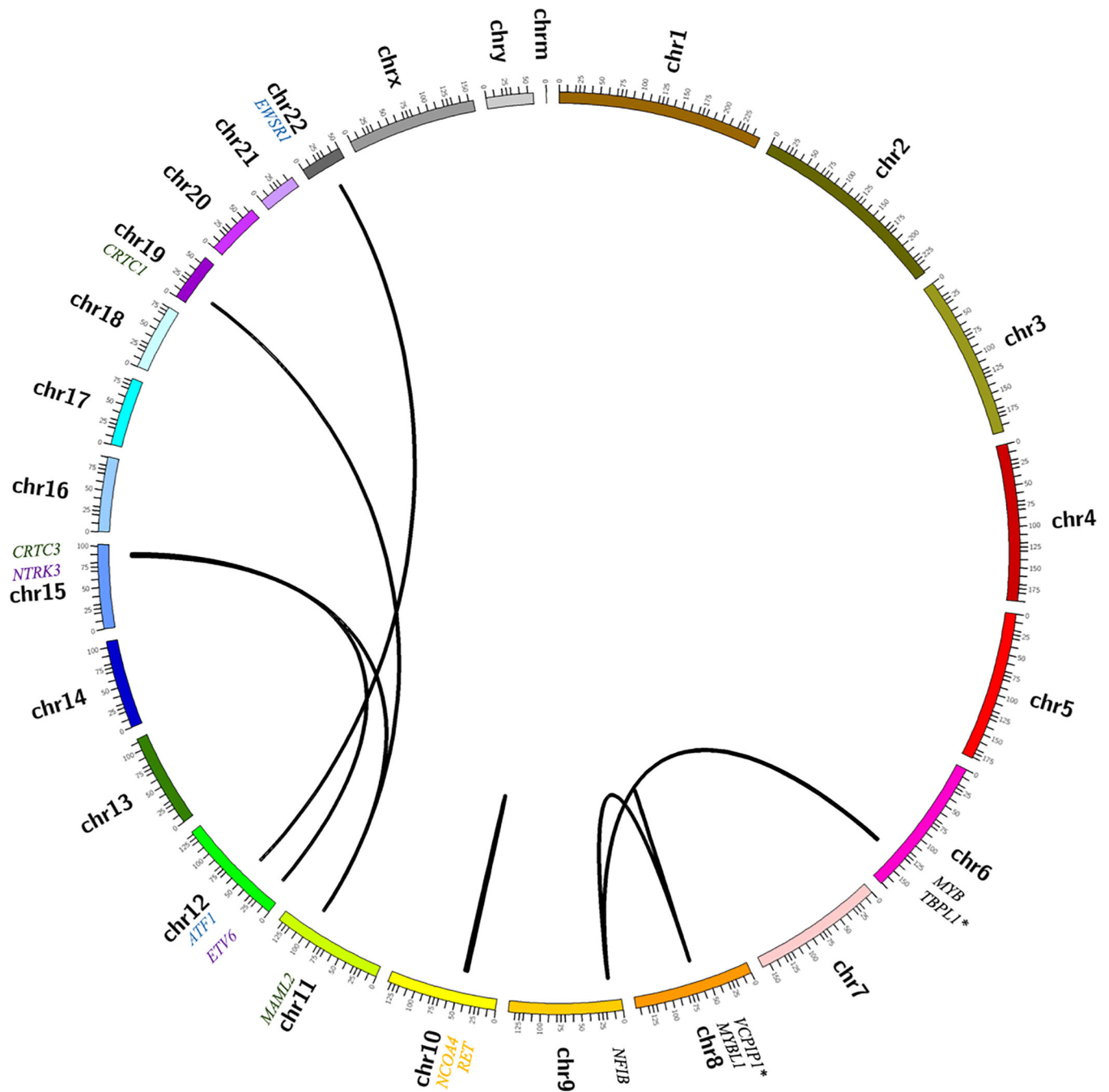


Figure 1.

Circos plots summarizing molecular alterations detected by RNA sequencing in cohort of salivary gland tumors. (A) Pleomorphic adenoma and carcinoma ex-pleomorphic adenoma. (B) Less common salivary gland neoplasms, including mucoepidermoid carcinoma (green), adenoid cystic carcinoma (black), hyalinizing clear cell carcinoma (blue), secretory carcinoma (purple) and intraductal carcinoma (orange). Novel fusion partners are indicated by an asterisk (*).

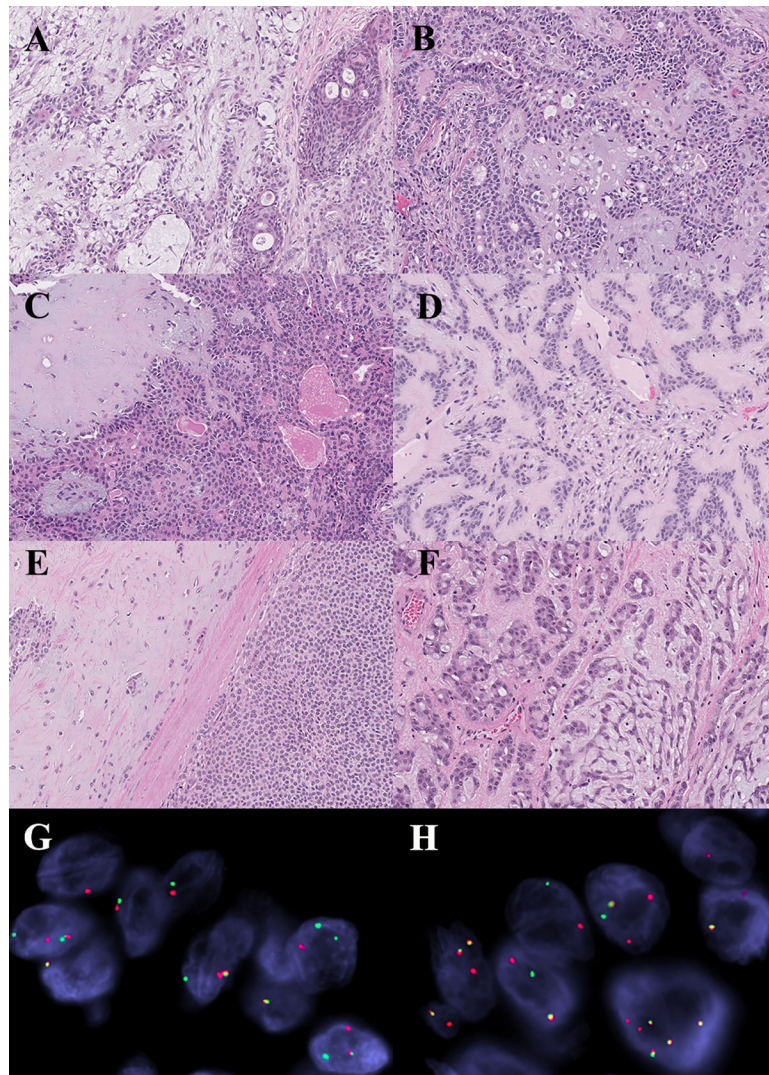


Figure 2. Histomorphologic and molecular correlates in pleomorphic adenoma. (A) Tumor with *CTNNB1-PLAG1* fusion gene. (B) Tumor lacking fusion gene. (C) Tumor with novel *DSTN-PLAG1* fusion product. (D) Tumor with novel *NTF3-PLAG1* fusion product. Note: there is no significant morphologic differences amongst the tumors with known and novel fusions, or those that are fusion negative. (E) Carcinoma ex-pleomorphic adenoma with *FBXO32-PLAG1* fusion gene. (F-H) Carcinoma ex-pleomorphic adenoma with *PLAG1-NFIB* fusion gene. (G) FISH demonstrating *PLAG1* rearrangement. (H) FISH demonstrating *NFIB* rearrangement.

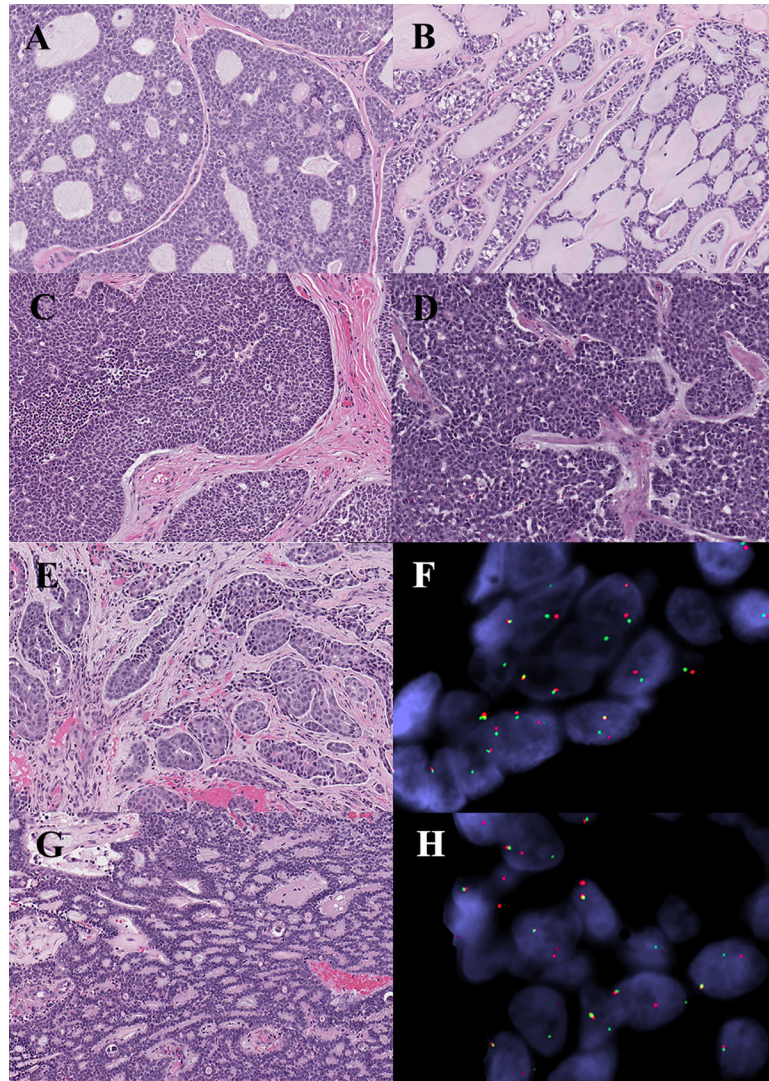


Figure 3.

Histomorphologic and molecular correlates in adenoid cystic carcinoma. (A) Tumor with *MYB-NFIB* fusion product. (B) Tumor lacking identifiable fusion gene with prototypic cribriform morphology. (C) Tumor with *MYB-NFIB* fusion gene with solid growth. (D) Tumor with *MYB-NFIB* fusion gene and high-grade transformation. (E-F) Tumor with novel *NFIB-TBPL1* fusion gene fusion, and tubular architecture. (F) FISH demonstrating *NFIB* rearrangement. (G-H) Tumor with novel *MYBL1-VCPIP1* fusion gene, and features mimicking polymorphous adenocarcinoma. (H) FISH demonstrating *MYBL1* rearrangement.

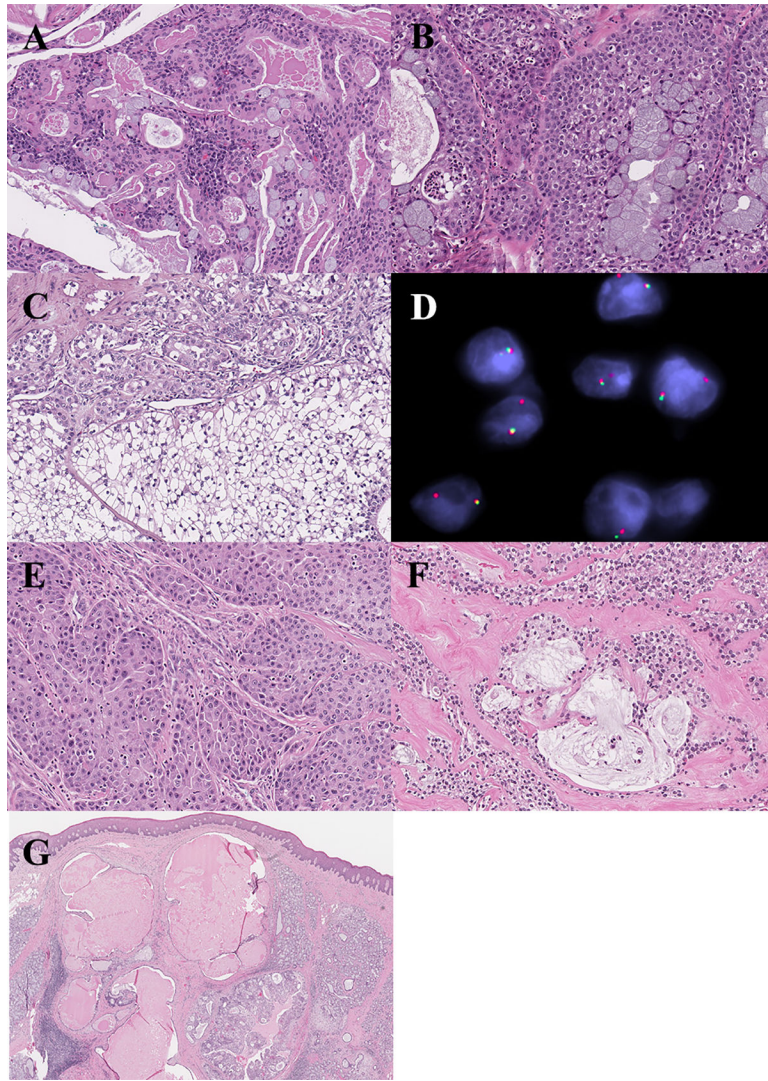


Figure 4. Mucoepidermoid carcinoma. (A) Tumor with *CRTC1-MAML2* fusion gene. (B) Tumor lacking identifiable fusion, with classic morphology. (C-D) Clear cell variant with *CRTC3-MAML2* fusion product. (D) FISH demonstrating *MAML2* rearrangement. (E) Oncocytic variant with *CRTC1-MAML2*, and paucity of mucous cells. (F) Tumor with *CRTC1-MAML2* fusion gene, and clear cells embedded in hyalinized stroma mimicking hyalinizing clear cell carcinoma. (G) Tumor with *CRTC1-MAML2* fusion product, and predominantly cystic architecture, mimicking a benign cystic lesion on incisional biopsy. Classic morphology was observed only in the deep aspect of the resection specimen (inset).

Table 1.

Summary of clinical details. Abbreviations: *AcCC*: acinic cell carcinoma, *AdCC*: adenoid cystic carcinoma, *CA-ex-PA*: carcinoma ex pleomorphic adenoma, *HCCC*: hyalinizing clear cell carcinoma, *F*: female, *IC*: intraductal carcinoma, *LN*: lymph node, *M*: male, *MEC*: mucoepidermoid carcinoma, *NOS*: not otherwise specified, *SC*: secretory carcinoma, *SDC*: salivary duct carcinoma, *SMG*: submandibular gland.

Case	Diagnosis	Age (y)	Sex	Location	Tumor Size (cm)
1	PA	67	M	Parotid gland	4.6
2	PA	56	F	Parotid gland	3.6
3	PA	46	F	Parotid gland	2.1
4	PA	21	M	SMG	1.7
5	PA	43	F	Parotid gland	1.5
6	PA	53	M	Parotid gland	2.9
7	PA	38	F	Parotid gland	2.7
8	PA	59	F	Parotid gland	1.5
9	PA	26	M	Parotid gland	4.5
10	PA	31	F	Parotid gland	2.6
11	PA	77	F	Parotid gland	2.1
12	PA	36	F	Parotid gland	2.0
13	PA	52	F	SMG	1.2
14	PA	78	F	Parotid gland	3.1
15	PA	48	F	Parotid gland	2.1
16	PA	48	F	Parotid gland	1.6
17	PA	20	M	SMG	1.8
18	PA	9	M	Oral cavity	2.5
19	PA	17	M	Oral cavity	Unknown
20	PA	77	F	SMG	Unknown
21	PA	42	M	Oral cavity	1.6
22	PA	63	M	Parotid gland	3.2
23	PA	49	M	Parotid gland	4.0
24	PA	79	F	Parotid gland	2.8
25	PA	53	M	Parotid gland	3.0
26	PA	26	F	Unknown	Unknown
27	PA	33	F	Oral Cavity	Unknown
28	CA-ex-PA	62	M	Parotid gland	3.6
29	CA-ex-PA	68	M	Parotid gland	3.6
30	CA-ex-PA	58	F	Parotid gland	1.7
31	CA-ex-PA	69	F	SMG	4.5
32	CA-ex-PA	49	M	Parotid gland	4.5
33	CA-ex-PA	55	F	Parotid gland	5.9
34	SDC-ex-PA	65	F	Parotid gland	1.7

Case	Diagnosis	Age (y)	Sex	Location	Tumor Size (cm)
35	AdCC	28	M	Nasal cavity	3.5
36	AdCC	38	F	Nasal cavity	Unknown
37	AdCC	39	F	Nasopharynx	Unknown
38	AdCC	55	F	Oral cavity	Unknown
39	AdCC	70	M	Ethmoid sinus	Unknown
40	AdCC	72	M	Orbit	Unknown
41	AdCC	66	F	Maxillary sinus	1.7
42	AdCC	53	F	Oral cavity	Unknown
43	AdCC	51	F	Oral cavity	1.1
44	AdCC	71	F	Oral cavity	1.9
45	AdCC	56	F	SMG	1.8
46	AdCC	38	M	Lacrimal gland	Unknown
47	AdCC	59	F	Larynx	Unknown
48	AdCC	59	M	Oral cavity	5.9
49	AdCC	62	M	Parotid gland	3.9
50	AdCC	59	M	Brain	Unknown
51	AdCC	96	F	Oral cavity	Unknown
52	AdCC	74	M	Nasal cavity	Unknown
53	AdCC	53	F	Vertebrae	Unknown
54	AdCC	50	M	Oral cavity	Unknown
55	MEC	53	M	Parotid gland	2.3
56	MEC	33	F	Parotid gland	3.1
57	MEC	64	F	Oral cavity	3
58	MEC	84	F	Oral cavity	Unknown
59	MEC	57	M	Oral cavity	Unknown
60	MEC	25	M	Parotid gland	4.7
61	MEC	62	F	Parotid gland	3.5
62	MEC	65	M	Oral cavity	2.1
63	MEC	63	F	Parotid gland	1.2
64	MEC	44	F	Parotid gland	1.5
65	MEC	80	F	Parotid gland	0.6
66	MEC	61	F	Parotid gland	5.9
67	MEC	63	F	Oral cavity	0.8
68	MEC	35	F	Neck, NOS	Unknown
69	AcCC	20	F	Parotid gland	1.9
70	AcCC	68	F	Parotid gland	0.6
71	AcCC	59	F	Parotid gland	2
72	AcCC	69	M	Parotid gland	3.9
73	AcCC	46	F	Parotid gland	1.7

Case	Diagnosis	Age (y)	Sex	Location	Tumor Size (cm)
74	HCCC	42	M	Base of tongue	3.8
75	HCCC	54	F	Oral cavity	0.7
76	HCCC	71	M	Cervical LN	Unknown
77	SC	56	F	Parotid gland	1.8
78	SC	48	F	Parotid gland	Unknown
79	SDC	63	F	Parotid gland	1.9
80	IC	68	M	Parotid gland	1.5

Author Manuscript

Author Manuscript

Author Manuscript

Author Manuscript

Table 2:

Summary of molecular results. *AcCC*: acinic cell carcinoma, *AdCC*: adenoid cystic carcinoma, *CA-ex-PA*: carcinoma ex pleomorphic adenoma, *HCCC*: hyalinizing clear cell carcinoma, *IC*: intraductal carcinoma, *MEC*: mucoepidermoid carcinoma, *N/A*: not assessed, *PA*: pleomorphic adenoma, *SC*: secretory carcinoma, *SDC*: salivary duct carcinoma.

Case	Diagnosis	RNA-Seq	5' Gene (NCBI Reference)	3' Gene (NCBI Reference)	FISH
1	PA	<i>PRB2-TAF15</i> *	-	-	<i>TAF15</i> -
2	PA	Negative	-	-	N/A
3	PA	<i>NPM1-PRB2</i> *	9 of 11 (NM_002520.6)	3 of 4 (NM_006248.3)	Negative
4	PA	<i>DSTN-PLAG1</i>	1 of 4 (NM_006870.3)	3 of 5 (NM_002655.2)	<i>PLAG1</i> -
5	PA	<i>CTNNB1-PLAG1</i>	1 of 15 (NM_001904.3)	2 of 5 (NM_002655.2)	N/A
6	PA	<i>CTNNB1-PLAG1</i>	1 of 15 (NM_001904.3)	3 of 5 (NM_002655.2)	N/A
7	PA	<i>HMGA2-WIF1</i>	3 of 5 (NM_003483.4)	10 of 10 (NM_007191.4)	N/A
8	PA	<i>HMGA2-WIF1</i>	3 of 5 (NM_003483.4)	10 of 10 (NM_007191.4)	N/A
9	PA	Negative	-	-	N/A
10	PA	<i>CTNNB1-PLAG1</i>	1 of 15 (NM_001904.3)	3 of 5 (NM_002655.2)	N/A
11	PA	<i>NTF3-PLAG1</i>	1 of 2 (NM_001102654.1)	3 of 5 (NM_002655.2)	<i>PLAG1</i> +
12	PA	<i>CTNNB1-PLAG1</i>	1 of 15 (NM_001904.3)	3 of 5 (NM_002655.2)	N/A
13	PA	<i>LIFR-PLAG1</i>	1 of 20 (NM_002310.5)	3 of 5 (NM_002655.2)	N/A
14	PA	Negative	-	-	N/A
15	PA	Negative	-	-	N/A
16	PA	Negative	-	-	N/A
17	PA	Negative	-	-	N/A
18	PA	<i>ACTA2-PLAG1</i>	1 of 9 (NM_001613.4)	3 of 5 (NM_002655.3)	N/A
19	PA	<i>NCALD-PLAG1</i>	1 of 4 (NM_032041.2)	3 of 5 (NM_002655.2)	N/A
20	PA	<i>HMGA2-WIF1</i>	3 of 5 (NM_003483.4)	3 of 10 (NM_007191.4)	N/A
21	PA	<i>CTNNB1-PLAG1</i>	1 of 15 (NM_001904.3)	3 of 5 (NM_002655.2)	N/A
22	PA	<i>CHCHD7-PLAG1</i>	3 of 5 (NM_001011667.2)	3 of 5 (NM_002655.2)	N/A
23	PA	Negative	-	-	N/A
24	PA	<i>NCALD-PLAG1</i>	1 of 4 (NM_032041.2)	3 of 5 (NM_002655.2)	<i>PLAG1</i> +
25	PA	<i>CTNNB1-PLAG1</i>	1 of 15 (NM_001904.3)	3 of 5 (NM_002655.2)	N/A
26	PA	<i>FBXO32-PLAG1</i>	1 of 9 (NM_058229.3)	3 of 5 (NM_002655.2)	<i>PLAG1</i> +
27	PA	<i>NCALD-PLAG1</i>	1 of 4 (NM_032041.2)	3 of 5 (NM_002655.2)	<i>PLAG1</i> +
28	CA-ex-PA	<i>FGFR1-PLAG1</i>	2 of 18 (NM_023110.2)	3 of 5 (NM_002655.2)	N/A
29	CA-ex-PA	<i>FBXO32-PLAG1</i>	1 of 9 (NM_058229.3)	3 of 5 (NM_002655.2)	<i>PLAG1</i> +
30	CA-ex-PA	<i>HMGA2-NFIB</i>	3 of 5 (NM_003483.4)	9 of 11 (NM_001190737.1)	N/A
31	CA-ex-PA	<i>MEG3-PLAG1</i>	1 of 7 (NR_002766.2)	3 of 5 (NM_002655.2)	<i>PLAG1</i> +
32	CA-ex-PA	<i>PLAG1-NFIB</i>	1 of 5 (NM_002655.2)	3 of 11 (NM_001190737.1)	<i>PLAG1</i> +, <i>NFIB</i> +
33	CA-ex-PA	<i>HMGA2-CNOT2</i>	2 of 5 (NM_003483.4)	12 of 16 (NM_001199303.1)	<i>HMGA2</i> amplification

Case	Diagnosis	RNA-Seq	5' Gene (NCBI Reference)	3' Gene (NCBI Reference)	FISH
34	SDC-ex-PA	Negative	-	-	N/A
35	AdCC	<i>MYB-NFIB</i>	13 of 16 (NM_001130173.1)	11 of 11 (NM_001190737.1)	N/A
36	AdCC	<i>MYBL1-NFIB</i>	14 of 16 (NM_001080416.3)	9 of 11 (NM_001190737.1)	N/A
37	AdCC	<i>MYB-NFIB</i>	15 of 16 (NM_001130173.1)	11 of 11 (NM_001190737.1)	N/A
38	AdCC	<i>MYBL1-NFIB</i>	8 of 16 (NM_001080416.3)	11 of 11 (NM_001190737.1)	N/A
39	AdCC	<i>MYB-NFIB</i>	15 of 16 (NM_001130173.1)	10 of 11 (NM_001282787.1)	N/A
40	AdCC	<i>MYB-NFIB</i>	15 of 16 (NM_001130173.1)	11 of 11 (NM_001190737.1)	N/A
41	AdCC	<i>MYB-NFIB</i>	15 of 16 (NM_001130173.1)	11 of 11 (NM_001190737.1)	N/A
42	AdCC	<i>MYB-NFIB</i>	13 of 16 (NM_001130173.1)	11 of 11 (NM_001190737.1)	N/A
43	AdCC	<i>MYB-NFIB</i>	8 of 16 (NM_001130173.1)	10 of 11 (NM_001282787.1)	N/A
44	AdCC	<i>MYBL1-NFIB</i>	8 of 16 (NM_001080416.3)	10 of 11 (NM_001282787.1)	N/A
45	AdCC	Negative	-	-	N/A
46	AdCC	<i>MYB-NFIB</i>	8 of 16 (NM_001130173.1)	11 of 11 (NM_001190737.1)	N/A
47	AdCC	<i>MYB-NFIB</i>	15 of 16 (NM_001130173.1)	11 of 11 (NM_001190737.1)	N/A
48	AdCC	<i>MYB-NFIB</i>	8 of 16 (NM_001130173.1)	11 of 11 (NM_001190737.1)	N/A
49	AdCC	<i>MYB-NFIB</i>	9 of 16 (NM_001130173.1)	11 of 11 (NM_001190737.1)	N/A
50	AdCC	<i>MYBL1-NFIB</i>	8 of 16 (NM_001080416.3)	9 of 11 (NM_001190737.1)	N/A
51	AdCC	<i>NFIB-TBPL1</i>	10 of 11 (NM_001190737.1)	7 of 7 (NM_001253676.1)	<i>NFIB</i> +
52	AdCC	<i>MYBL1-NFIB</i>	12 of 16 (NM_001080416.3)	2 of 11 (NM_001190737.1)	N/A
53	AdCC	<i>MYB-NFIB</i>	13 of 16 (NM_001130173.1)	11 of 11 (NM_001190737.1)	N/A
54	AdCC	<i>MYBL1-VCPIP1</i>	9 of 16 (NM_001080416.3)	3 of 3 (NM_025054.4)	<i>MYBL1</i> +
55	MEC	Negative	-	-	<i>MAML2</i> +
56	MEC	<i>CRTC1-MAML2</i>	2 of 14 (NM_015321.2)	1 of 5 (NM_032427.3)	<i>MAML2</i> +
57	MEC	Negative	-	-	<i>MAML2</i> +
58	MEC	<i>CRTC3-MAML2</i>	2 of 15 (NM_022769.4)	2 of 5 (NM_032427.3)	<i>MAML2</i> +
59	MEC	Negative	-	-	Negative
60	MEC	<i>CRTC1-MAML2</i>	2 of 14 (NM_015321.2)	1 of 5 (NM_032427.3)	<i>MAML2</i> +
61	MEC	<i>CRTC1-MAML2</i>	1 of 14 (NM_015321.2)	2 of 5 (NM_032427.3)	<i>MAML2</i> +
62	MEC	Negative	-	-	<i>MAML2</i> +
63	MEC	<i>CRTC1-MAML2</i>	1 of 14 (NM_015321.2)	2 of 5 (NM_032427.3)	<i>MAML2</i> +
64	MEC	Negative	-	-	Negative
65	MEC	<i>CRTC3-MAML2</i>	2 of 15 (NM_022769.4)	2 of 5 (NM_032427.3)	<i>MAML2</i> +
66	MEC	<i>CRTC1-MAML2</i>	1 of 14 (NM_015321.2)	2 of 5 (NM_032427.3)	<i>MAML2</i> +
67	MEC	<i>CRTC1-MAML2</i>	1 of 14 (NM_015321.2)	2 of 5 (NM_032427.3)	<i>MAML2</i> +
68	MEC	<i>CRTC3-MAML2</i>	2 of 15 (NM_022769.4)	2 of 5 (NM_032427.3)	Negative
69	AcCC	Negative	-	-	N/A
70	AcCC	Negative	-	-	N/A
71	AcCC	Negative	-	-	N/A
72	AcCC	Negative	-	-	N/A

Case	Diagnosis	RNA-Seq	5' Gene (NCBI Reference)	3' Gene (NCBI Reference)	FISH
73	AcCC	Negative			N/A
74	HCCC	<i>EWSR1-ATF1</i>	12 of 18 (NM_013986.3)	3 of 7 (NM_005171.4)	N/A
75	HCCC	Negative	-	-	N/A
76	HCCC	<i>EWSR1-ATF1</i>	14 of 18 (NM_013986.3)	5 of 7 (NM_005171.4)	N/A
77	SC	<i>ETV6-NTRK3</i>	5 of 8 (NM_001987.4)	15 of 20 (NM_001012338.2)	N/A
78	SC	<i>ETV6-NTRK3</i>	5 of 8 (NM_001987.4)	15 of 20 (NM_001012338.2)	N/A
79	SDC	<i>RAPGEF6-ACSL6</i>	1 of 29 (NM_001164386.1)	2 of 21 (NM_015256.3)	N/A
80	IC	<i>NCOA4-RET</i>	8 of 12 (NM_001145260.1)	12 of 20 (NM_020975.5)	N/A

Stochastic events highlighted by an asterisk (*).

Author Manuscript

Author Manuscript

Author Manuscript

Author Manuscript